Measurement of Antiproton Production in p-He Collisions at $\sqrt{s_{\mathrm{NN}}} = 110$ GeV

R. Aaij *et al.*[*]
(LHCb Collaboration)

(Received 21 August 2018; revised manuscript received 9 October 2018; published 29 November 2018)

The cross section for prompt antiproton production in collisions of protons with an energy of 6.5 TeV incident on helium nuclei at rest is measured with the LHCb experiment from a data set corresponding to an integrated luminosity of 0.5 nb^{-1}. The target is provided by injecting helium gas into the LHC beam line at the LHCb interaction point. The reported results, covering antiproton momenta between 12 and 110 GeV/c, represent the first direct determination of the antiproton production cross section in p-He collisions, and impact the interpretation of recent results on antiproton cosmic rays from space-borne experiments.

DOI: 10.1103/PhysRevLett.121.222001

The antiproton fraction in cosmic rays has been long recognized as a sensitive indirect probe for exotic astrophysical sources of antimatter, such as dark matter annihilation [1–5]. A substantial improvement in experimental accuracy for the measurement of the antiproton, $\bar{p}$, over proton, p, flux ratio has recently been achieved by the space-borne PAMELA [6] and AMS-02 [7] experiments. Antiproton production in spallation of cosmic rays in the interstellar medium, which is mainly composed of hydrogen and helium, is expected to produce a $\bar{p}/p$ flux ratio of $\mathcal{O}(10^{-4})$. The observed excess of $\bar{p}$ yields over current predictions for the known production sources [8–11] can still be accommodated within the current uncertainties. In the 10–100 GeV $\bar{p}$ energy range, these uncertainties are dominated by the limited knowledge of the $\bar{p}$ production cross section in the relevant processes. To date, no direct measurements of $\bar{p}$ production in p-He collisions have been made, and no data are available at a nucleon-nucleon center-of-mass (c.m.) energy of $\sqrt{s_{\mathrm{NN}}} \sim 100$ GeV, relevant for the production of cosmic antiprotons above 10 GeV [12].

This Letter reports the first measurement of prompt $\bar{p}$ production in p-He collisions carried out with the LHCb experiment at CERN using a proton beam with an energy of 6.5 TeV impinging on a helium gas target. The forward geometry and particle identification (PID) capabilities of the LHCb detector are exploited to reconstruct antiprotons with momentum, p, ranging from 12 to 110 GeV/c and transverse momentum, p_T, between 0.4 and 4.0 GeV/c. The integrated luminosity is determined from the yield of elastically scattered atomic electrons.

The LHCb detector is a single-arm forward spectrometer covering the pseudorapidity range $2 < \eta < 5$, described in detail in Refs. [13,14], conceived for heavy-flavor physics in pp collisions at the CERN LHC. The momentum of charged particles is measured to better than 1.0% for $p < 110$ GeV/c. The silicon-strip vertex locator (VELO), which surrounds the nominal pp interaction region, allows the measurement of the minimum distance of a track to a primary vertex (PV), the impact parameter (IP), with a resolution of $(15 + 29/p_{\mathrm{T}})$ μm, where p_{T} is in GeV/c. Different types of charged hadrons are distinguished using two ring-imaging Cherenkov detectors (RICH) [15], whose acceptance and performance define the $\bar{p}$ kinematic range accessible to this study. The first RICH detector has an inner acceptance limited to $\eta < 4.4$ and is used to identify antiprotons with momenta between 12 and 60 GeV/c. The second detector covers the range $3 < \eta < 5$ and can actively identify antiprotons with momenta between 30 and 110 GeV/c. The scintillating-pad (SPD) detector and the electromagnetic calorimeter (ECAL) included in the calorimeter system are also used in this study.

The SMOG (system for measuring overlap with gas) device [16,17] enables the injection of noble gases with pressure of $\mathcal{O}(10^{-7})$ mbar in the beam pipe section crossing the VELO, allowing LHCb to operate as a fixed-target experiment. This analysis is performed on data specifically acquired for this measurement in May 2016. Helium gas was injected when the two beams circulating in the LHC accelerator [18] consisted of a small number, between 52 and 56, of proton bunches. The proton-beam energy of 6.5 TeV corresponds to $\sqrt{s_{\mathrm{NN}}} = 110.5$ GeV. In the proton-nucleon c.m. frame,

[*]Full author list given at the end of the article.

the LHCb acceptance corresponds to central and backward rapidities $-2.8 < y^* < 0.2$, and $\bar{p}$ production can be studied for values of x-Feynman, the ratio of the $\bar{p}$ longitudinal momentum to its maximal value, comprised between -0.24 and 0.

To avoid background from pp collisions, the events used for this measurement were recorded when a bunch in the beam pointing toward LHCb crosses the nominal interaction region without a corresponding colliding bunch in the other beam. The online event selection consists of a hardware stage, which requires activity in the SPD detector, and a software stage requiring at least one reconstructed track in the VELO. An unbiased control sample of randomly selected events is acquired independently of this online selection.

Simulated data samples are generated for p-He collisions with EPOS-LHC [19], and for pe^- normalization events with ESEPP [20]. The interaction of the generated particles with the detector, and its response, are implemented using the GEANT4 toolkit [21] as described in Ref. [22]. Simulated collisions are uniformly distributed along the nominal beam direction z in the range $-1000 < z < +300$ mm, where $z = 0$ mm is the nominal collision point.

Events with antiproton candidates must have a reconstructed primary vertex within the fiducial region $-700 < z_{\rm PV} < +100$ mm, where high reconstruction efficiencies are achieved for both p-He and pe^- collisions. The PV position must be compatible with the beam profile and events must have fewer than 5 tracks reconstructed in the VELO with negative pseudorapidity. This selection is $(99.8 \pm 0.2)\%$ efficient for simulated reconstructed p-He vertices, while suppressing vertices from interactions with material, decays, and particle showers produced in beam-gas collisions occurring upstream of the VELO. The overlap of these backgrounds with a p-He collision, an effect not accounted for by the simulation, causes an additional inefficiency of $(2.3 \pm 0.2)\%$, measured using the unbiased control sample. The PV reconstruction efficiency for the signal events is estimated from simulation and varies with $z_{\rm PV}$ from 66% in the most upstream region to 97% around $z_{\rm PV} = 0$ mm. This efficiency is sensitive to the PV track multiplicity, the angular distribution of primary tracks, and the average position and profile of the beam. Imperfections in these simulated distributions are accounted for by weighting simulated events to improve the agreement with the distributions observed in data. From the resulting variations of the PV reconstruction efficiency, a relative systematic uncertainty is assigned, ranging from 1.6% to 3.3%, depending on the $\bar{p}$ kinematics.

Antiproton candidates are selected from negatively charged tracks within the acceptance of at least one of the RICH detectors. Additionally, $\bar{p}$ candidates are required to originate from the primary vertex by requiring $\chi^2_{\rm IP} < 12$, where $\chi^2_{\rm IP}$ is defined as the difference in the vertex-fit χ^2 of the PV reconstructed with and without the track under consideration. The reconstruction efficiency for prompt antiprotons, $\epsilon_{\rm rec}$, including the detector acceptance and the tracking efficiency, is determined from simulation in three-dimensional bins of p, p_T, and $z_{\rm PV}$. The width of the momentum bins increases as a power law of p to have approximately an equal number of candidates in each of 18 bins. Ten p_T bins are chosen with the same criterion, while 12 uniform bins are used in $z_{\rm PV}$. Bins in which $\epsilon_{\rm rec}$ is below 25% are not used in order to reduce systematic uncertainties, effectively shortening the $z_{\rm PV}$ fiducial region for kinematic bins at the edges of the detector acceptance. The average value of $\epsilon_{\rm rec}$ in the remaining bins is 61%. The tracking efficiency obtained from the simulation is corrected by a factor determined from calibration samples in pp-collision data. This correction factor is consistent with unity in all kinematic bins within its systematic uncertainty of 0.8% [23]. The $z_{\rm PV}$ dependence of the tracking efficiency is checked using $K^0_S \to \pi^+\pi^-$ decays in the p-He sample where one of the tracks is reconstructed without using VELO information. No significant differences between data and simulation are observed. A systematic uncertainty, varying between 1.0% and 4.0% depending on η, accounts for $\bar{p}$ hadronic interactions in the detector material, whose rate is known with 10% accuracy [23]. The efficiency of the $\chi^2_{\rm IP}$ requirement is parametrized as a function of p_T and p, averaging to 96.1%, with a 1.0% uncertainty from the parametrization accuracy. The online selection efficiency is unity, within 10^{-5}, as determined from the unbiased control sample.

Based on studies of simulated p-He collisions, the sample of negatively charged tracks is dominated by π^-, K^-, and $\bar{p}$ hadrons. In a small fraction of cases, 1.7% in the simulation, tracks do not correspond to the trajectories of real charged particles and are labeled as fake tracks. Particle identification is based on the response of the RICH detectors, from which two quantities are determined: the difference between the log likelihood of the proton and pion hypotheses, $\mathrm{DLL}_{p\pi}$, and that between the proton and kaon hypotheses, DLL_{pK} [15]. Three sets of templates for each particle species are determined from simulation, from p-He data, and from pp data collected in 2016. The p-He calibration samples consist of selected $K^0_S \to \pi^+\pi^-$ decays for pions, $\Lambda \to p\pi^-(\bar{\Lambda} \to \bar{p}\pi^+)$ for (anti)protons, and $\phi \to K^+K^-$ for kaons. Calibration samples in pp data also include $D^{*\pm} \to \overset{(-)}{D}{}^0(K^\mp\pi^\pm)\pi^\pm$ decays. Simulation is used for the template of fake tracks.

Two methods are used to determine the $\bar{p}$ fraction in each kinematic bin: a two-dimensional binned extended-maximum-likelihood fit, illustrated in Fig. 1, and a cut-and-count method [24], which uses exclusive high-purity samples selected with tight requirements for each particle species. The probability P_{ij} that a candidate of species i is classified as species j is obtained from

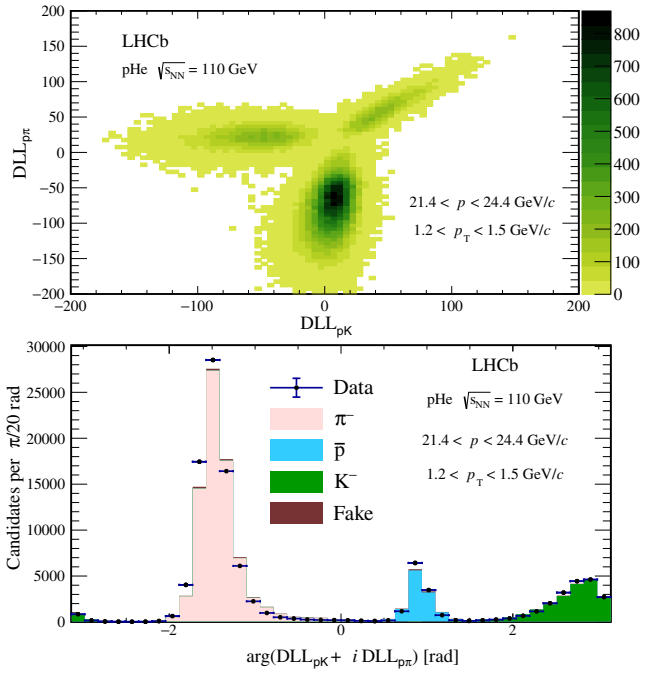

FIG. 1. Two-dimensional template fit to the PID distribution of negatively charged tracks for a particular bin ($21.4 < p < 24.4$ GeV/c, $1.2 < p_T < 1.5$ GeV/c). The ($\mathrm{DLL_{pK}}$, $\mathrm{DLL_{p\pi}}$) distribution, shown in the top plot, is fitted to determine the relative contribution of π^-, K^-, and $\bar{p}$ particles, using simulation to determine the template distributions and the fraction of fake tracks (which are barely visible). In the bottom plot, the result of the fit is projected into the variable arg ($\mathrm{DLL_{pK}} + i\mathrm{DLL_{p\pi}}$).

the templates. The 4×4 P_{ij} matrix is then inverted to derive the yield of each particle species. For each kinematic bin, the central value for the $\bar{p}$ fraction is obtained from the average of the two methods using the templates from simulation, while half the difference is used to estimate the systematic uncertainty. Bias from the imperfections of the simulated RICH response, which are visible in Fig. 1, is estimated from the average differences among the results using the three available template sets, which are used to assign an additional uncertainty, correlated among bins. The total uncertainty is typically a few percent, although larger uncertainties affect the bins at the edges of the detector acceptance.

In the simulation, the nonprompt antiprotons surviving the χ^2_{IP} requirement constitute a fraction of the selected $\bar{p}$ sample varying between 1% and 3% depending on p_T. These are due to hyperon decays, in 90% of cases, or secondary interactions. This fraction is corrected by a factor 1.5 ± 0.3, to account for differences between simulation and data as determined in the region of the χ^2_{IP} distribution dominated by hyperon decays. The resulting correction to the $\bar{p}$ yield averages to -2.4%.

Collisions on the residual gas in the LHC beam vacuum, with a pressure of $\mathcal{O}(10^{-9})$ mbar and unknown composition, can contribute to the $\bar{p}$ yield. Residual-gas analysis, performed in the absence of beam, indicates that the contamination is $\mathcal{O}(1)\%$ and is dominated by hydrogen. To evaluate this background source, including a possible beam-induced component, a control sample of beam-gas collisions was acquired before injection of the helium gas. Data collected with and without helium gas have the same vacuum pumping configuration and thus identical residual gas composition and pressure. The yield of selected events in data without helium gas, scaled according to the corresponding number of protons on target, is subtracted from the result leading to an average correction of $(-0.6 \pm 0.1)\%$, where the uncertainty accounts for the background variation over time. The average PV track multiplicity is found to be smaller in collisions without injected gas, confirming that the residual gas is dominated by hydrogen.

Since the injected gas pressure is not precisely known, the integrated luminosity of the data sample is determined from the yield of electrons from elastic scattering of the proton beam. Scattered electrons are simulated in the polar angle range $3 < \theta < 27$ mrad, outside of which they cannot be reconstructed in LHCb. The corresponding cross section is calculated to be 184.8 ± 1.8 μb [20], where the uncertainty is due to the proton form factors and radiative corrections. Scattered electrons are selected from events with a single reconstructed track. The electron candidate is required to have $p < 15$ GeV/c, $p_T < 0.12$ GeV/c, a polar angle in the range $11 < \theta < 21$ mrad, and to originate from the fiducial region. The longitudinal position of the scattering vertex $z_{\mathrm{pe^-}}$ is determined from the position of minimum approach to the beam line, with a resolution of 9 cm. The track reconstruction efficiency in the selected $z_{\mathrm{pe^-}}$ and θ ranges is determined from simulation to be 16.3%. A loose requirement is placed on the energy deposited in the ECAL to identify the track as an electron. Background events that could mimic this signature are expected to be mostly soft nuclear collisions where the initial nucleons do not dissociate, and the detected particle is produced by a colorless exchange of gluons or photons. Since the products of this process must be charge-symmetric, the background yield is determined from events with a single positron candidate.

Background is further suppressed by two multivariate classifiers, implemented using a boosted decision tree algorithm [25]. The first exploits the geometric and kinematic properties of the candidate electron. The second uses multiplicity variables to veto any extra activity in the event. In both cases the classifiers are trained using pe^- simulated events for the signal and single-positron events from data for the background. Loose requirements are placed on the response of the boosted decision tree discriminants, with a combined efficiency of 96% for simulated pe^- events. The overlap of a pe^- event with another beam-gas interaction causes an additional inefficiency, measured to be

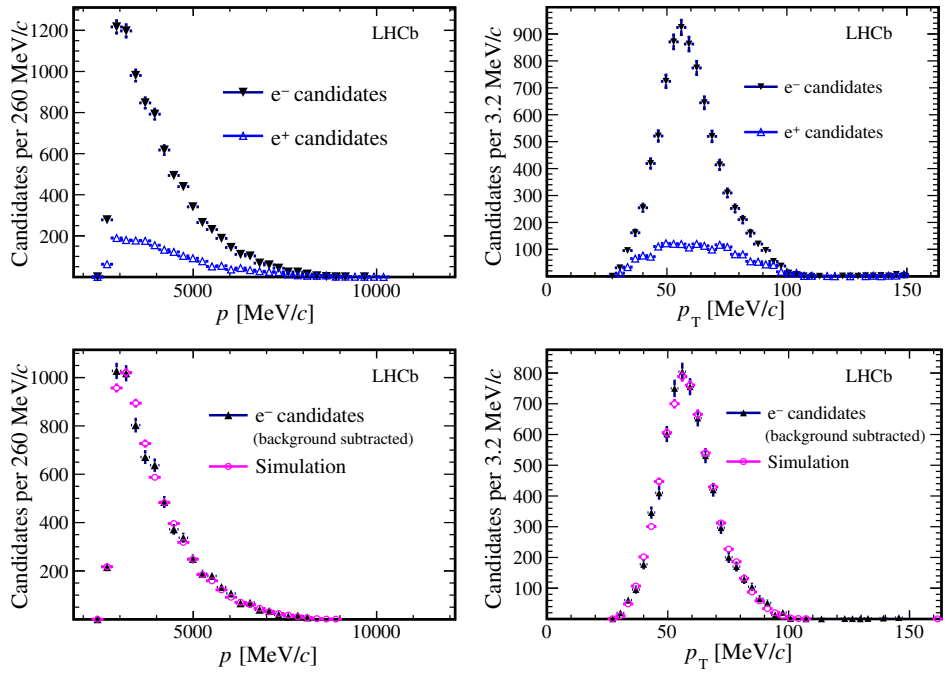

FIG. 2. Distributions of (left) momentum and (right) transverse momentum for (top) single electron and single positron candidates, and (bottom) background-subtracted electron candidates, compared with the distributions in simulation, which are normalized to the data yield.

$(9.4 \pm 0.7)\%$ in the unbiased control sample. A possible charge asymmetry of the background, estimated from the EPOS simulation, leads to a systematic uncertainty of 1.9%. As is done for the $\bar{p}$ candidates, the unbiased control events are used to measure the online selection efficiency, $(98.3 \pm 0.3)\%$, and the data without helium gas are used to determine the contribution from scattering on residual gas, $(1.0 \pm 0.3)\%$.

The momentum distributions of the selected candidates are shown in Fig. 2, where a good agreement with the simulated pe^- signal is observed after background subtraction. The low reconstruction efficiency, due to the fact that the observed electrons are predominantly produced at the edges of the LHCb acceptance and are subject to relevant energy losses by bremsstrahlung when crossing the detector material, is the major source of systematic uncertainty on the luminosity. The stability of the result is checked against additional requirements on the most critical variables, notably the number of reconstructed VELO hits and the azimuthal angle, whose distribution is strongly affected by the spectrometer magnetic field. The largest variation of the result, a relative 5.0%, is assigned as systematic uncertainty on the electron reconstruction efficiency. Taking also into account an uncertainty of 2.3% from the beam and VELO simulated geometry, the total systematic uncertainty on the luminosity is 6.0%.

The integrated p-He luminosity is determined from the efficiency-corrected yield, divided by the product of the pe^- cross section and the helium atomic number. Gas ionization effects are found to be negligible. Avoiding any assumption on the z dependence of the gas density, the integrated luminosity is calculated with 12 z_{pe^-} bins across the fiducial region, resulting in $484 \pm 7 \pm 29\ \mu\text{b}^{-1}$, where the first uncertainty is statistical and the second is systematic. From the knowledge of the number of delivered protons, the target gas pressure is found to be

TABLE I. Relative uncertainties on the $\bar{p}$ production cross section. The ranges refer to the variation among kinematic bins.

Statistical	
$\bar{p}$ yields	0.5%–11% (<2% for most bins)
Luminosity	1.5%–2.3%
Correlated systematic	
Luminosity	6.0%
Event and PV selection	0.3%
PV reconstruction	0.4%–2.9%
Tracking	1.3%–4.1%
Nonprompt background	0.3%–0.5%
Target purity	0.1%
PID	3.0%–6.0%
Uncorrelated systematic	
Tracking	1.0%
IP cut efficiency	1.0%
PV reconstruction	1.6%
PID	0%–36% (<5% for most bins)
Simulated sample size	0.4%–11% (<2% for most bins)

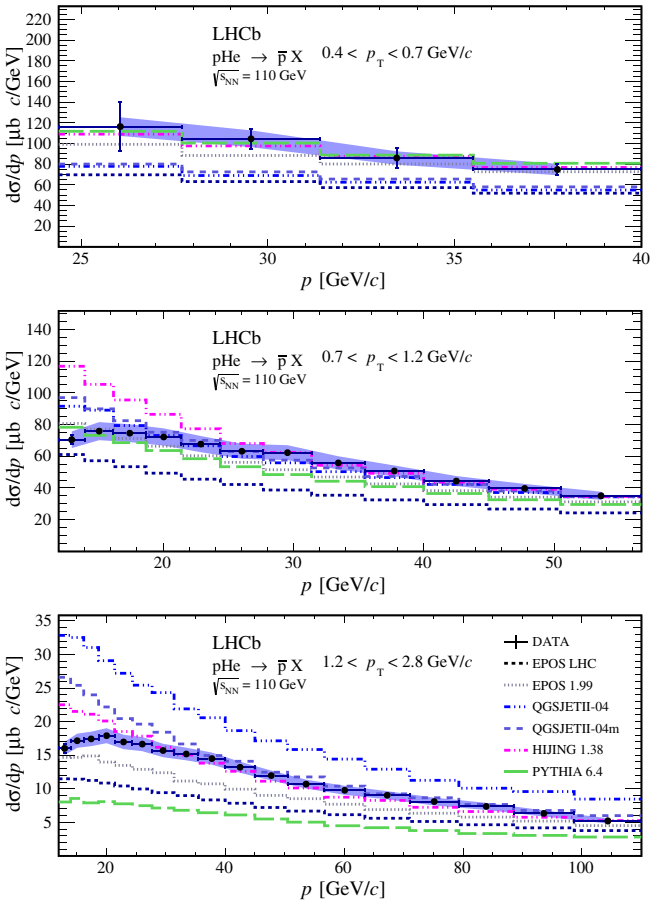

FIG. 3. Antiproton production cross section per He nucleus as a function of momentum, integrated over various p_T regions. The data points are compared with predictions from theoretical models. The uncertainties on the data points are uncorrelated only, while the shaded area indicates the correlated uncertainty.

2.6×10^{-7} mbar, which is compatible with the expected helium pressure.

Table I presents the list of uncertainties on the $\bar{p}$ cross-section measurement, categorized into correlated and uncorrelated sources among kinematic bins. The correlated systematic uncertainty is dominated by the uncertainty on the luminosity determination. The net effect of migration between kinematic bins due to resolution effects is found to be negligible. A major difference between the fixed-target configuration and the standard pp-collision data taking in LHCb is the extension of the luminous region. As a consequence, the result is checked to be independent of z_{PV} within the quoted uncertainty in all kinematic bins. Furthermore, the results do not show any significant dependence on the time of data taking.

The $\bar{p}$ production cross section is determined in each kinematic bin from a sample of 33.7×10^6 reconstructed p-He collisions, yielding 1.5×10^6 antiprotons as determined from the PID analysis. In Fig. 3, the results, integrated in different kinematic regions, are compared with the prediction of several models: EPOS-LHC [19], the pre-LHC EPOS version 1.99 [26], HIJING 1.38 [27], the QGSJET model II-04 [28] and its low-energy extension QGSJETII-04m, motivated by $\bar{p}$ production in cosmic rays [29]. The results are also compared with the PYTHIA6.4 [30] prediction for $2 \times [\sigma(pp \to \bar{p}X) + \sigma(pn \to \bar{p}X)]$, not including nuclear effects. The shapes are well reproduced except at low rapidity, and the absolute $\bar{p}$ yields deviate by up to a factor of 2. Numerical values for the double-differential cross section $d^2\sigma/dpdp_{\mathrm{T}}$ in each kinematic bin are available in the Supplemental Material [31].

The total yield of p-He inelastic collisions which are visible in LHCb is determined from the yield of reconstructed primary vertices and is found to be compatible with EPOS-LHC: $\sigma_{\mathrm{vis}}^{\mathrm{LHCb}}/\sigma_{\mathrm{vis}}^{\mathrm{EPOS-LHC}} = 1.08 \pm 0.07 \pm 0.03$, where the first uncertainty is due to the luminosity and the second to the PV reconstruction efficiency. The result indicates that the significant excess of $\bar{p}$ production over the EPOS-LHC prediction, visible in Fig. 3, is mostly due to the $\bar{p}$ multiplicity.

In summary, using a p-He collision data sample, corresponding to an integrated luminosity of 0.5 nb^{-1}, the LHCb Collaboration has performed the first measurement of antiproton production in p-He collisions. The precision is limited by systematic effects and is better than a relative 10% for most kinematic bins, well below the spread among models describing $\bar{p}$ production in nuclear collisions. The energy scale, $\sqrt{s_{\mathrm{NN}}} = 110$ GeV, and the measured range of the antiproton kinematic spectrum are crucial for interpreting the precise $\bar{p}$ cosmic ray measurements from the PAMELA and AMS-02 experiments by improving the precision of the secondary $\bar{p}$ cosmic ray flux prediction [11,32].

We are grateful to our colleagues from the cosmic ray community, O. Adriani, F. Donato, L. Bonechi and A. Tricomi, for suggesting this measurement, to T. Pierog and S. Ostapchenko for their advice on the theoretical models for antiproton production, and to B. Ward and A. V. Gramolin for their advice on the model and uncertainty for pe^- scattering. We express our gratitude to our colleagues in the CERN accelerator departments for the excellent performance of the LHC. We thank the technical and administrative staff at the LHCb institutes. We acknowledge support from CERN and from the national agencies: CAPES, CNPq, FAPERJ and FINEP (Brazil); MOST and NSFC (China); CNRS/IN2P3 (France); BMBF, DFG and MPG (Germany); INFN (Italy); NWO (Netherlands); MNiSW and NCN (Poland); MEN/IFA (Romania); MSHE (Russia); MinECo (Spain); SNSF and SER (Switzerland); NASU (Ukraine); STFC (United Kingdom); NSF (USA). We acknowledge the computing resources that are provided by CERN, IN2P3 (France), KIT and DESY (Germany), INFN (Italy), SURF (Netherlands), PIC (Spain), GridPP (United Kingdom), RRCKI and

Yandex LLC (Russia), CSCS (Switzerland), IFIN-HH (Romania), CBPF (Brazil), PL-GRID (Poland) and OSC (USA). We are indebted to the communities behind the multiple open-source software packages on which we depend. Individual groups or members have received support from AvH Foundation (Germany); EPLANET, Marie Skłodowska-Curie Actions and ERC (European Union); ANR, Labex P2IO and OCEVU, and Région Auvergne-Rhóne-Alpes (France); Key Research Program of Frontier Sciences of CAS, CAS PIFI, and the Thousand Talents Program (China); RFBR, RSF and Yandex LLC (Russia); GVA, XuntaGal and GENCAT (Spain); the Royal Society and the Leverhulme Trust (United Kingdom); Laboratory Directed Research and Development program of LANL (USA).

[1] T. K. Gaisser and E. H. Levy, Phys. Rev. D **10**, 1731 (1974).
[2] G. Steigman, Annu. Rev. Astron. Astrophys. **14**, 339 (1976).
[3] J. Silk and M. Srednicki, Phys. Rev. Lett. **53**, 624 (1984).
[4] F. W. Stecker, S. Rudaz, and T. F. Walsh, Phys. Rev. Lett. **55**, 2622 (1985).
[5] J. S. Hagelin and G. L. Kane, Nucl. Phys. **B263**, 399 (1986).
[6] O. Adriani *et al.* (PAMELA Collaboration), JETP Lett. **96**, 621 (2013).
[7] M. Aguilar *et al.* (AMS Collaboration), Phys. Rev. Lett. **117**, 091103 (2016).
[8] M. di Mauro, F. Donato, A. Goudelis, and P. D. Serpico, Phys. Rev. D **90**, 085017 (2014).
[9] G. Giesen, M. Boudaud, Y. Génolini, V. Poulin, M. Cirelli, P. Salati, and P. D. Serpico, J. Cosmol. Astropart. Phys. 09 (2015) 023.
[10] R. Kappl, A. Reinert, and M. W. Winkler, J. Cosmol. Astropart. Phys. 10 (2015) 034.
[11] A. Reinert and M. W. Winkler, J. Cosmol. Astropart. Phys. 01 (2018) 055.
[12] F. Donato, M. Korsmeier, and M. Di Mauro, Phys. Rev. D **96**, 043007 (2017).
[13] A. A. Alves, Jr. *et al.* (LHCb Collaboration), J. Instrum. **3**, S08005 (2008).
[14] R. Aaij *et al.* (LHCb Collaboration), Int. J. Mod. Phys. A **30**, 1530022 (2015).
[15] M. Adinolfi *et al.*, Eur. Phys. J. C **73**, 2431 (2013).
[16] C. Barschel, Precision luminosity measurement at LHCb with beam-gas imaging, Ph.D. thesis, RWTH Aachen University, 2014; Report No. CERN-THESIS-2013-301, https://cds.cern.ch/record/1693671.
[17] R. Aaij *et al.* (LHCb Collaboration), J. Instrum. **9**, P12005 (2014).
[18] L. Evans and P. Bryant, J. Instrum. **3**, S08001 (2008).
[19] T. Pierog, I. Karpenko, J. M. Katzy, E. Yatsenko, and K. Werner, Phys. Rev. C **92**, 034906 (2015).
[20] A. V. Gramolin, V. S. Fadin, A. L. Feldman, R. E. Gerasimov, D. M. Nikolenko, I. A. Rachek, and D. K. Toporkov, J. Phys. G **41**, 115001 (2014).
[21] J. Allison *et al.* (Geant4 Collaboration), IEEE Trans. Nucl. Sci. **53**, 270 (2006); S. Agostinelli *et al.* (Geant4 Collaboration), Nucl. Instrum. Methods, Phys. Res., Sect. A **506**, 250 (2003).
[22] M. Clemencic, G. Corti, S. Easo, C. R. Jones, S. Miglioranzi, M. Pappagallo, and P. Robbe, J. Phys. Conf. Ser. **331**, 032023 (2011).
[23] R. Aaij *et al.* (LHCb Collaboration), J. Instrum. **10**, P02007 (2015).
[24] R. Aaij *et al.* (LHCb Collaboration), Eur. Phys. J. C **72**, 2168 (2012).
[25] Y. Freund and R. E. Schapire, J. Comput. Syst. Sci. **55**, 119 (1997).
[26] T. Pierog and K. Werner, Nucl. Phys. B, Proc. Suppl. **196**, 102 (2009).
[27] M. Gyulassy and X.-N. Wang, Comput. Phys. Commun. **83**, 307 (1994).
[28] S. Ostapchenko, Phys. Rev. D **83**, 014018 (2011).
[29] M. Kachelriess, I. V. Moskalenko, and S. S. Ostapchenko, Astrophys. J. **803**, 54 (2015).
[30] T. Sjöstrand, S. Mrenna, and P. Skands, J. High Energy Phys. 05 (2006) 026.
[31] See Supplemental Material at http://link.aps.org/supplemental/10.1103/PhysRevLett.121.222001 for the numerical results of this study.
[32] M. Korsmeier, F. Donato, and M. Di Mauro, Phys. Rev. D **97**, 103019 (2018).

R. Aaij,[28] C. Abellán Beteta,[45] B. Adeva,[42] M. Adinolfi,[49] C. A. Aidala,[74] Z. Ajaltouni,[5] S. Akar,[60] P. Albicocco,[19] J. Albrecht,[10] F. Alessio,[43] M. Alexander,[54] A. Alfonso Albero,[41] G. Alkhazov,[34] P. Alvarez Cartelle,[56] A. A. Alves Jr,[42] S. Amato,[2] S. Amerio,[24] Y. Amhis,[7] L. An,[3] L. Anderlini,[17] G. Andreassi,[44] M. Andreotti,[16] J. E. Andrews,[61] R. B. Appleby,[57] F. Archilli,[28] P. d'Argent,[12] J. Arnau Romeu,[6] A. Artamonov,[40] M. Artuso,[62] K. Arzymatov,[38] E. Aslanides,[6] M. Atzeni,[45] B. Audurier,[23] S. Bachmann,[12] J. J. Back,[51] S. Baker,[56] V. Balagura,[7,a] W. Baldini,[16] A. Baranov,[38] R. J. Barlow,[57] S. Barsuk,[7] W. Barter,[57] F. Baryshnikov,[71] V. Batozskaya,[32] B. Batsukh,[62] V. Battista,[44] A. Bay,[44] J. Beddow,[54] F. Bedeschi,[25] I. Bediaga,[1] A. Beiter,[62] L. J. Bel,[28] S. Belin,[23] N. Beliy,[64] V. Bellee,[44] N. Belloli,[21,b] K. Belous,[40] I. Belyaev,[35,43] E. Ben-Haim,[8] G. Bencivenni,[19] S. Benson,[28] S. Beranek,[9] A. Berezhnoy,[36] R. Bernet,[45] D. Berninghoff,[12] E. Bertholet,[8] A. Bertolin,[24] C. Betancourt,[45] F. Betti,[15,43] M. O. Bettler,[50] M. van Beuzekom,[28] Ia. Bezshyiko,[45] S. Bhasin,[49] J. Bhom,[30] S. Bifani,[48] P. Billoir,[8] A. Birnkraut,[10] A. Bizzeti,[17,c] M. Bjørn,[58] M. P. Blago,[43] T. Blake,[51] F. Blanc,[44] S. Blusk,[62] D. Bobulska,[54] V. Bocci,[27] O. Boente Garcia,[42] T. Boettcher,[59] A. Bondar,[39,d] N. Bondar,[34]

S. Borghi,[57,43] M. Borisyak,[38] M. Borsato,[42] F. Bossu,[7] M. Boubdir,[9] T. J. V. Bowcock,[55] C. Bozzi,[16,43] S. Braun,[12] M. Brodski,[43] J. Brodzicka,[30] A. Brossa Gonzalo,[51] D. Brundu,[23] E. Buchanan,[49] A. Buonaura,[45] C. Burr,[57] A. Bursche,[23] J. Buytaert,[43] W. Byczynski,[43] S. Cadeddu,[23] H. Cai,[65] R. Calabrese,[16,e] R. Calladine,[48] M. Calvi,[21,b] M. Calvo Gomez,[41,f] A. Camboni,[41,f] P. Campana,[19] D. H. Campora Perez,[43] L. Capriotti,[15] A. Carbone,[15,g] G. Carboni,[26] R. Cardinale,[20,h] A. Cardini,[23] P. Carniti,[21,b] L. Carson,[53] K. Carvalho Akiba,[2] G. Casse,[55] L. Cassina,[21] M. Cattaneo,[43] G. Cavallero,[20,h] R. Cenci,[25,i] D. Chamont,[7] M. G. Chapman,[49] M. Charles,[8] Ph. Charpentier,[43] G. Chatzikonstantinidis,[48] M. Chefdeville,[4] V. Chekalina,[38] C. Chen,[3] S. Chen,[23] S.-G. Chitic,[43] V. Chobanova,[42] M. Chrzaszcz,[43] A. Chubykin,[34] P. Ciambrone,[19] X. Cid Vidal,[42] G. Ciezarek,[43] P. E. L. Clarke,[53] M. Clemencic,[43] H. V. Cliff,[50] J. Closier,[43] V. Coco,[43] J. A. B. Coelho,[7] J. Cogan,[6] E. Cogneras,[5] L. Cojocariu,[33] P. Collins,[43] T. Colombo,[43] A. Comerma-Montells,[12] A. Contu,[23] G. Coombs,[43] S. Coquereau,[41] G. Corti,[43] M. Corvo,[16,e] C. M. Costa Sobral,[51] B. Couturier,[43] G. A. Cowan,[53] D. C. Craik,[59] A. Crocombe,[51] M. Cruz Torres,[1] R. Currie,[53] C. D'Ambrosio,[43] F. Da Cunha Marinho,[2] C. L. Da Silva,[75] E. Dall'Occo,[28] J. Dalseno,[49] A. Danilina,[35] A. Davis,[3] O. De Aguiar Francisco,[43] K. De Bruyn,[43] S. De Capua,[57] M. De Cian,[44] J. M. De Miranda,[1] L. De Paula,[2] M. De Serio,[14,j] P. De Simone,[19] C. T. Dean,[54] D. Decamp,[4] L. Del Buono,[8] B. Delaney,[50] H.-P. Dembinski,[11] M. Demmer,[10] A. Dendek,[31] D. Derkach,[38] O. Deschamps,[5] F. Desse,[7] F. Dettori,[55] B. Dey,[66] A. Di Canto,[43] P. Di Nezza,[19] S. Didenko,[71] H. Dijkstra,[43] F. Dordei,[43] M. Dorigo,[43,k] A. Dosil Suárez,[42] L. Douglas,[54] A. Dovbnya,[46] K. Dreimanis,[55] L. Dufour,[28] G. Dujany,[8] P. Durante,[43] J. M. Durham,[75] D. Dutta,[57] R. Dzhelyadin,[40] M. Dziewiecki,[12] A. Dziurda,[30] A. Dzyuba,[34] S. Easo,[52] U. Egede,[56] V. Egorychev,[35] S. Eidelman,[39,d] S. Eisenhardt,[53] U. Eitschberger,[10] R. Ekelhof,[10] L. Eklund,[54] S. Ely,[62] A. Ene,[33] S. Escher,[9] S. Esen,[28] T. Evans,[60] A. Falabella,[15] N. Farley,[48] S. Farry,[55] D. Fazzini,[21,43,b] L. Federici,[26] P. Fernandez Declara,[43] A. Fernandez Prieto,[42] F. Ferrari,[15] L. Ferreira Lopes,[44] F. Ferreira Rodrigues,[2] M. Ferro-Luzzi,[43] S. Filippov,[37] R. A. Fini,[14] M. Fiorini,[16,e] M. Firlej,[31] C. Fitzpatrick,[44] T. Fiutowski,[31] F. Fleuret,[7,a] M. Fontana,[23,43] F. Fontanelli,[20,h] R. Forty,[43] V. Franco Lima,[55] M. Frank,[43] C. Frei,[43] J. Fu,[22,l] W. Funk,[43] C. Färber,[43] M. Féo Pereira Rivello Carvalho,[28] E. Gabriel,[53] A. Gallas Torreira,[42] D. Galli,[15,g] S. Gallorini,[24] S. Gambetta,[53] Y. Gan,[3] M. Gandelman,[2] P. Gandini,[22] Y. Gao,[3] L. M. Garcia Martin,[73] B. Garcia Plana,[42] J. García Pardiñas,[45] J. Garra Tico,[50] L. Garrido,[41] D. Gascon,[41] C. Gaspar,[43] L. Gavardi,[10] G. Gazzoni,[5] D. Gerick,[12] E. Gersabeck,[57] M. Gersabeck,[57] T. Gershon,[51] D. Gerstel,[6] Ph. Ghez,[4] S. Gianì,[44] V. Gibson,[50] O. G. Girard,[44] L. Giubega,[33] K. Gizdov,[53] V. V. Gligorov,[8] D. Golubkov,[35] A. Golutvin,[56,71] A. Gomes,[1,m] I. V. Gorelov,[36] C. Gotti,[21,b] E. Govorkova,[28] J. P. Grabowski,[12] R. Graciani Diaz,[41] L. A. Granado Cardoso,[43] E. Graugés,[41] E. Graverini,[45] G. Graziani,[17] A. Grecu,[33] R. Greim,[28] P. Griffith,[23] L. Grillo,[57] L. Gruber,[43] B. R. Gruberg Cazon,[58] O. Grünberg,[68] C. Gu,[3] E. Gushchin,[37] Yu. Guz,[40,43] T. Gys,[43] C. Göbel,[63] T. Hadavizadeh,[58] C. Hadjivasiliou,[5] G. Haefeli,[44] C. Haen,[43] S. C. Haines,[50] B. Hamilton,[61] X. Han,[12] T. H. Hancock,[58] S. Hansmann-Menzemer,[12] N. Harnew,[58] S. T. Harnew,[49] T. Harrison,[55] C. Hasse,[43] M. Hatch,[43] J. He,[64] M. Hecker,[56] K. Heinicke,[10] A. Heister,[10] K. Hennessy,[55] L. Henry,[73] E. van Herwijnen,[43] M. Heß,[68] A. Hicheur,[2] R. Hidalgo Charman,[57] D. Hill,[58] M. Hilton,[57] P. H. Hopchev,[44] W. Hu,[66] W. Huang,[64] Z. C. Huard,[60] W. Hulsbergen,[28] T. Humair,[56] M. Hushchyn,[38] D. Hutchcroft,[55] D. Hynds,[28] P. Ibis,[10] M. Idzik,[31] P. Ilten,[48] K. Ivshin,[34] R. Jacobsson,[43] J. Jalocha,[58] E. Jans,[28] A. Jawahery,[61] F. Jiang,[3] M. John,[58] D. Johnson,[43] C. R. Jones,[50] C. Joram,[43] B. Jost,[43] N. Jurik,[58] S. Kandybei,[46] M. Karacson,[43] J. M. Kariuki,[49] S. Karodia,[54] N. Kazeev,[38] M. Kecke,[12] F. Keizer,[50] M. Kelsey,[62] M. Kenzie,[50] T. Ketel,[29] E. Khairullin,[38] B. Khanji,[43] C. Khurewathanakul,[44] K. E. Kim,[62] T. Kirn,[9] S. Klaver,[19] K. Klimaszewski,[32] T. Klimkovich,[11] S. Koliiev,[47] M. Kolpin,[12] R. Kopecna,[12] P. Koppenburg,[28] I. Kostiuk,[28] S. Kotriakhova,[34] M. Kozeiha,[5] L. Kravchuk,[37] M. Kreps,[51] F. Kress,[56] P. Krokovny,[39,d] W. Krupa,[31] W. Krzemien,[32] W. Kucewicz,[30,n] M. Kucharczyk,[30] V. Kudryavtsev,[39,d] A. K. Kuonen,[44] T. Kvaratskheliya,[35,43] D. Lacarrere,[43] G. Lafferty,[57] A. Lai,[23] D. Lancierini,[45] G. Lanfranchi,[19] C. Langenbruch,[9] T. Latham,[51] C. Lazzeroni,[48] R. Le Gac,[6] A. Leflat,[36] J. Lefrançois,[7] R. Lefèvre,[5] F. Lemaitre,[43] O. Leroy,[6] T. Lesiak,[30] B. Leverington,[12] P.-R. Li,[64] T. Li,[3] Z. Li,[62] X. Liang,[62] T. Likhomanenko,[70] R. Lindner,[43] F. Lionetto,[45] V. Lisovskyi,[7] X. Liu,[3] D. Loh,[51] A. Loi,[23] I. Longstaff,[54] J. H. Lopes,[2] G. H. Lovell,[50] C. Lucarelli,[18] D. Lucchesi,[24,o] M. Lucio Martinez,[42] A. Lupato,[24] E. Luppi,[16,e] O. Lupton,[43] A. Lusiani,[25] X. Lyu,[64] F. Machefert,[7] F. Maciuc,[33] V. Macko,[44] P. Mackowiak,[10] S. Maddrell-Mander,[49] O. Maev,[34,43] K. Maguire,[57] D. Maisuzenko,[34] M. W. Majewski,[31] S. Malde,[58] B. Malecki,[30] A. Malinin,[70] T. Maltsev,[39,d] G. Manca,[23,p] G. Mancinelli,[6] D. Marangotto,[22,l] J. Maratas,[5,q] J. F. Marchand,[4] U. Marconi,[15] S. Mariani,[18] C. Marin Benito,[7] M. Marinangeli,[44] P. Marino,[44] J. Marks,[12] P. J. Marshall,[55] G. Martellotti,[27] M. Martin,[6] M. Martinelli,[43] D. Martinez Santos,[42] F. Martinez Vidal,[73] A. Massafferri,[1] M. Materok,[9] R. Matev,[43] A. Mathad,[51] Z. Mathe,[43] C. Matteuzzi,[21] A. Mauri,[45] E. Maurice,[7,a] B. Maurin,[44] A. Mazurov,[48] M. McCann,[56,43] A. McNab,[57] R. McNulty,[13]

J. V. Mead,[55] B. Meadows,[60] C. Meaux,[6] F. Meier,[10] N. Meinert,[68] D. Melnychuk,[32] M. Merk,[28] A. Merli,[22,l] E. Michielin,[24] D. A. Milanes,[67] E. Millard,[51] M.-N. Minard,[4] L. Minzoni,[16,e] D. S. Mitzel,[12] A. Mogini,[8] J. Molina Rodriguez,[1,r] T. Mombächer,[10] I. A. Monroy,[67] S. Monteil,[5] M. Morandin,[24] G. Morello,[19] M. J. Morello,[25,s] O. Morgunova,[70] J. Moron,[31] A. B. Morris,[6] R. Mountain,[62] F. Muheim,[53] M. Mulder,[28] C. H. Murphy,[58] D. Murray,[57] A. Mödden,[10] D. Müller,[43] J. Müller,[10] K. Müller,[45] V. Müller,[10] P. Naik,[49] T. Nakada,[44] R. Nandakumar,[52] A. Nandi,[58] T. Nanut,[44] I. Nasteva,[2] M. Needham,[53] N. Neri,[22] S. Neubert,[12] N. Neufeld,[43] M. Neuner,[12] R. Newcombe,[56] T. D. Nguyen,[44] C. Nguyen-Mau,[44,t] S. Nieswand,[9] R. Niet,[10] N. Nikitin,[36] A. Nogay,[70] N. S. Nolte,[43] D. P. O'Hanlon,[15] A. Oblakowska-Mucha,[31] V. Obraztsov,[40] S. Ogilvy,[19] R. Oldeman,[23,p] C. J. G. Onderwater,[69] A. Ossowska,[30] J. M. Otalora Goicochea,[2] P. Owen,[45] A. Oyanguren,[73] P. R. Pais,[44] T. Pajero,[25,s] A. Palano,[14] M. Palutan,[19,43] G. Panshin,[72] A. Papanestis,[52] M. Pappagallo,[53] L. L. Pappalardo,[16,e] W. Parker,[61] C. Parkes,[57] G. Passaleva,[17,43] A. Pastore,[14] M. Patel,[56] C. Patrignani,[15,g] A. Pearce,[43] A. Pellegrino,[28] G. Penso,[27] M. Pepe Altarelli,[43] S. Perazzini,[43] D. Pereima,[35] P. Perret,[5] L. Pescatore,[44] K. Petridis,[49] A. Petrolini,[20,h] A. Petrov,[70] S. Petrucci,[53] M. Petruzzo,[22,l] B. Pietrzyk,[4] G. Pietrzyk,[44] M. Pikies,[30] M. Pili,[58] D. Pinci,[27] J. Pinzino,[43] F. Pisani,[43] A. Piucci,[12] V. Placinta,[33] S. Playfer,[53] J. Plews,[48] M. Plo Casasus,[42] F. Polci,[8] M. Poli Lener,[19] A. Poluektov,[51] N. Polukhina,[71,u] I. Polyakov,[62] E. Polycarpo,[2] G. J. Pomery,[49] S. Ponce,[43] A. Popov,[40] D. Popov,[48,11] S. Poslavskii,[40] C. Potterat,[2] E. Price,[49] J. Prisciandaro,[42] C. Prouve,[49] V. Pugatch,[47] A. Puig Navarro,[45] H. Pullen,[58] G. Punzi,[25,i] W. Qian,[64] J. Qin,[64] R. Quagliani,[8] B. Quintana,[5] B. Rachwal,[31] J. H. Rademacker,[49] M. Rama,[25] M. Ramos Pernas,[42] M. S. Rangel,[2] F. Ratnikov,[38,v] G. Raven,[29] M. Ravonel Salzgeber,[43] M. Reboud,[4] F. Redi,[44] S. Reichert,[10] A. C. dos Reis,[1] F. Reiss,[8] C. Remon Alepuz,[73] Z. Ren,[3] V. Renaudin,[7] S. Ricciardi,[52] S. Richards,[49] K. Rinnert,[55] P. Robbe,[7] A. Robert,[8] A. B. Rodrigues,[44] E. Rodrigues,[60] J. A. Rodriguez Lopez,[67] M. Roehrken,[43] S. Roiser,[43] A. Rollings,[58] V. Romanovskiy,[40] A. Romero Vidal,[42] M. Rotondo,[19] M. S. Rudolph,[62] T. Ruf,[43] J. Ruiz Vidal,[73] J. J. Saborido Silva,[42] N. Sagidova,[34] B. Saitta,[23,p] V. Salustino Guimaraes,[63] C. Sanchez Gras,[28] C. Sanchez Mayordomo,[73] B. Sanmartin Sedes,[42] R. Santacesaria,[27] C. Santamarina Rios,[42] M. Santimaria,[19] E. Santovetti,[26,w] G. Sarpis,[57] A. Sarti,[19,x] C. Satriano,[27,y] A. Satta,[26] M. Saur,[64] D. Savrina,[35,36] S. Schael,[9] M. Schellenberg,[10] M. Schiller,[54] H. Schindler,[43] M. Schmelling,[11] T. Schmelzer,[10] B. Schmidt,[43] O. Schneider,[44] A. Schopper,[43] H. F. Schreiner,[60] M. Schubiger,[44] M. H. Schune,[7] R. Schwemmer,[43] B. Sciascia,[19] A. Sciubba,[27,x] A. Semennikov,[35] E. S. Sepulveda,[8] A. Sergi,[48,43] N. Serra,[45] J. Serrano,[6] L. Sestini,[24] A. Seuthe,[10] P. Seyfert,[43] M. Shapkin,[40] Y. Shcheglov,[34] T. Shears,[55] L. Shekhtman,[39,d] V. Shevchenko,[70] E. Shmanin,[71] B. G. Siddi,[16] R. Silva Coutinho,[45] L. Silva de Oliveira,[2] G. Simi,[24,o] S. Simone,[14,j] I. Skiba,[16] N. Skidmore,[12] T. Skwarnicki,[62] M. W. Slater,[48] J. G. Smeaton,[50] E. Smith,[9] I. T. Smith,[53] M. Smith,[56] M. Soares,[15] l. Soares Lavra,[1] M. D. Sokoloff,[60] F. J. P. Soler,[54] B. Souza De Paula,[2] B. Spaan,[10] E. Spadaro Norella,[22,l] P. Spradlin,[54] F. Stagni,[43] M. Stahl,[12] S. Stahl,[43] P. Stefko,[44] S. Stefkova,[56] O. Steinkamp,[45] S. Stemmle,[12] O. Stenyakin,[40] M. Stepanova,[34] H. Stevens,[10] A. Stocchi,[7] S. Stone,[62] B. Storaci,[45] S. Stracka,[25] M. E. Stramaglia,[44] M. Straticiuc,[33] U. Straumann,[45] S. Strokov,[72] J. Sun,[3] L. Sun,[65] K. Swientek,[31] T. Szumlak,[31] M. Szymanski,[64] S. T'Jampens,[4] Z. Tang,[3] A. Tayduganov,[6] T. Tekampe,[10] G. Tellarini,[16] F. Teubert,[43] E. Thomas,[43] J. van Tilburg,[28] M. J. Tilley,[56] V. Tisserand,[5] M. Tobin,[31] S. Tolk,[43] L. Tomassetti,[16,e] D. Tonelli,[25] D. Y. Tou,[8] R. Tourinho Jadallah Aoude,[1] E. Tournefier,[4] M. Traill,[54] M. T. Tran,[44] A. Trisovic,[50] A. Tsaregorodtsev,[6] G. Tuci,[25,i] A. Tully,[50] N. Tuning,[28,43] A. Ukleja,[32] A. Usachov,[7] A. Ustyuzhanin,[38] U. Uwer,[12] A. Vagner,[72] V. Vagnoni,[15] A. Valassi,[43] S. Valat,[43] G. Valenti,[15] R. Vazquez Gomez,[43] P. Vazquez Regueiro,[42] S. Vecchi,[16] M. van Veghel,[28] J. J. Velthuis,[49] M. Veltri,[17,z] G. Veneziano,[58] A. Venkateswaran,[62] T. A. Verlage,[9] M. Vernet,[5] M. Veronesi,[28] N. V. Veronika,[13] M. Vesterinen,[58] J. V. Viana Barbosa,[43] D. Vieira,[64] M. Vieites Diaz,[42] H. Viemann,[68] X. Vilasis-Cardona,[41,f] A. Vitkovskiy,[28] M. Vitti,[50] V. Volkov,[36] A. Vollhardt,[45] D. Vom Bruch,[8] B. Voneki,[43] A. Vorobyev,[34] V. Vorobyev,[39,d] J. A. de Vries,[28] C. Vázquez Sierra,[28] R. Waldi,[68] J. Walsh,[25] J. Wang,[62] M. Wang,[3] Y. Wang,[66] Z. Wang,[45] D. R. Ward,[50] H. M. Wark,[55] N. K. Watson,[48] D. Websdale,[56] A. Weiden,[45] C. Weisser,[59] M. Whitehead,[9] J. Wicht,[51] G. Wilkinson,[58] M. Wilkinson,[62] I. Williams,[50] M. R. J. Williams,[57] M. Williams,[59] T. Williams,[48] F. F. Wilson,[52,43] J. Wimberley,[61] M. Winn,[7] J. Wishahi,[10] W. Wislicki,[32] M. Witek,[30] G. Wormser,[7] S. A. Wotton,[50] K. Wyllie,[43] D. Xiao,[66] Y. Xie,[66] A. Xu,[3] M. Xu,[66] Q. Xu,[64] Z. Xu,[3] Z. Xu,[4] Z. Yang,[3] Z. Yang,[61] Y. Yao,[62] L. E. Yeomans,[55] H. Yin,[66] J. Yu,[66,aa] X. Yuan,[62] O. Yushchenko,[40] K. A. Zarebski,[48] M. Zavertyaev,[11,u] D. Zhang,[66] L. Zhang,[3] W. C. Zhang,[3,bb] Y. Zhang,[7] A. Zhelezov,[12] Y. Zheng,[64] X. Zhu,[3] V. Zhukov,[9,36] J. B. Zonneveld,[53] and S. Zucchelli[15]

(LHCb Collaboration)

[1]Centro Brasileiro de Pesquisas Físicas (CBPF), Rio de Janeiro, Brazil
[2]Universidade Federal do Rio de Janeiro (UFRJ), Rio de Janeiro, Brazil
[3]Center for High Energy Physics, Tsinghua University, Beijing, China
[4]Univ. Grenoble Alpes, Univ. Savoie Mont Blanc, CNRS, IN2P3-LAPP, Annecy, France
[5]Clermont Université, Université Blaise Pascal, CNRS/IN2P3, LPC, Clermont-Ferrand, France
[6]Aix Marseille Univ, CNRS/IN2P3, CPPM, Marseille, France
[7]LAL, Univ. Paris-Sud, CNRS/IN2P3, Université Paris-Saclay, Orsay, France
[8]LPNHE, Sorbonne Université, Paris Diderot Sorbonne Paris Cité, CNRS/IN2P3, Paris, France
[9]I. Physikalisches Institut, RWTH Aachen University, Aachen, Germany
[10]Fakultät Physik, Technische Universität Dortmund, Dortmund, Germany
[11]Max-Planck-Institut für Kernphysik (MPIK), Heidelberg, Germany
[12]Physikalisches Institut, Ruprecht-Karls-Universität Heidelberg, Heidelberg, Germany
[13]School of Physics, University College Dublin, Dublin, Ireland
[14]INFN Sezione di Bari, Bari, Italy
[15]INFN Sezione di Bologna, Bologna, Italy
[16]INFN Sezione di Ferrara, Ferrara, Italy
[17]INFN Sezione di Firenze, Firenze, Italy
[18]Università di Firenze, Firenze, Italy
[19]INFN Laboratori Nazionali di Frascati, Frascati, Italy
[20]INFN Sezione di Genova, Genova, Italy
[21]INFN Sezione di Milano-Bicocca, Milano, Italy
[22]INFN Sezione di Milano, Milano, Italy
[23]INFN Sezione di Cagliari, Monserrato, Italy
[24]INFN Sezione di Padova, Padova, Italy
[25]INFN Sezione di Pisa, Pisa, Italy
[26]INFN Sezione di Roma Tor Vergata, Roma, Italy
[27]INFN Sezione di Roma La Sapienza, Roma, Italy
[28]Nikhef National Institute for Subatomic Physics, Amsterdam, Netherlands
[29]Nikhef National Institute for Subatomic Physics and VU University Amsterdam, Amsterdam, Netherlands
[30]Henryk Niewodniczanski Institute of Nuclear Physics Polish Academy of Sciences, Kraków, Poland
[31]AGH - University of Science and Technology, Faculty of Physics and Applied Computer Science, Kraków, Poland
[32]National Center for Nuclear Research (NCBJ), Warsaw, Poland
[33]Horia Hulubei National Institute of Physics and Nuclear Engineering, Bucharest-Magurele, Romania
[34]Petersburg Nuclear Physics Institute (PNPI), Gatchina, Russia
[35]Institute of Theoretical and Experimental Physics (ITEP), Moscow, Russia
[36]Institute of Nuclear Physics, Moscow State University (SINP MSU), Moscow, Russia
[37]Institute for Nuclear Research of the Russian Academy of Sciences (INR RAS), Moscow, Russia
[38]Yandex School of Data Analysis, Moscow, Russia
[39]Budker Institute of Nuclear Physics (SB RAS), Novosibirsk, Russia
[40]Institute for High Energy Physics (IHEP), Protvino, Russia
[41]ICCUB, Universitat de Barcelona, Barcelona, Spain
[42]Instituto Galego de Física de Altas Enerxías (IGFAE), Universidade de Santiago de Compostela, Santiago de Compostela, Spain
[43]European Organization for Nuclear Research (CERN), Geneva, Switzerland
[44]Institute of Physics, Ecole Polytechnique Fédérale de Lausanne (EPFL), Lausanne, Switzerland
[45]Physik-Institut, Universität Zürich, Zürich, Switzerland
[46]NSC Kharkiv Institute of Physics and Technology (NSC KIPT), Kharkiv, Ukraine
[47]Institute for Nuclear Research of the National Academy of Sciences (KINR), Kyiv, Ukraine
[48]University of Birmingham, Birmingham, United Kingdom
[49]H.H. Wills Physics Laboratory, University of Bristol, Bristol, United Kingdom
[50]Cavendish Laboratory, University of Cambridge, Cambridge, United Kingdom
[51]Department of Physics, University of Warwick, Coventry, United Kingdom
[52]STFC Rutherford Appleton Laboratory, Didcot, United Kingdom
[53]School of Physics and Astronomy, University of Edinburgh, Edinburgh, United Kingdom
[54]School of Physics and Astronomy, University of Glasgow, Glasgow, United Kingdom
[55]Oliver Lodge Laboratory, University of Liverpool, Liverpool, United Kingdom
[56]Imperial College London, London, United Kingdom
[57]School of Physics and Astronomy, University of Manchester, Manchester, United Kingdom
[58]Department of Physics, University of Oxford, Oxford, United Kingdom
[59]Massachusetts Institute of Technology, Cambridge, Massachusetts, USA

[60]University of Cincinnati, Cincinnati, Ohio, USA
[61]University of Maryland, College Park, Maryland, USA
[62]Syracuse University, Syracuse, New York, USA
[63]Pontifícia Universidade Católica do Rio de Janeiro (PUC-Rio), Rio de Janeiro, Brazil [associated with Institution Universidade Federal do Rio de Janeiro (UFRJ), Rio de Janeiro, Brazil]
[64]University of Chinese Academy of Sciences, Beijing, China (associated with Institution Center for High Energy Physics, Tsinghua University, Beijing, China)
[65]School of Physics and Technology, Wuhan University, Wuhan, China (associated with Institution Center for High Energy Physics, Tsinghua University, Beijing, China)
[66]Institute of Particle Physics, Central China Normal University, Wuhan, Hubei, China (associated with Institution Center for High Energy Physics, Tsinghua University, Beijing, China)
[67]Departamento de Fisica, Universidad Nacional de Colombia, Bogota, Colombia (associated with Institution LPNHE, Sorbonne Université, Paris Diderot Sorbonne Paris Cité, CNRS/IN2P3, Paris, France)
[68]Institut für Physik, Universität Rostock, Rostock, Germany (associated with Institution Physikalisches Institut, Ruprecht-Karls-Universität Heidelberg, Heidelberg, Germany)
[69]Van Swinderen Institute, University of Groningen, Groningen, Netherlands (associated with Institution Nikhef National Institute for Subatomic Physics, Amsterdam, Netherlands)
[70]National Research Centre Kurchatov Institute, Moscow, Russia [associated with Institution Institute of Theoretical and Experimental Physics (ITEP), Moscow, Russia]
[71]National University of Science and Technology "MISIS", Moscow, Russia [associated with Institution Institute of Theoretical and Experimental Physics (ITEP), Moscow, Russia]
[72]National Research Tomsk Polytechnic University, Tomsk, Russia [associated with Institution Institute of Theoretical and Experimental Physics (ITEP), Moscow, Russia]
[73]Instituto de Fisica Corpuscular, Centro Mixto Universidad de Valencia - CSIC, Valencia, Spain (associated with Institution ICCUB, Universitat de Barcelona, Barcelona, Spain)
[74]University of Michigan, Ann Arbor, USA (associated with Institution Syracuse University, Syracuse, New York, USA)
[75]Los Alamos National Laboratory (LANL), Los Alamos, USA (associated with Institution Syracuse University, Syracuse, New York, USA)

[a]Also at Laboratoire Leprince-Ringuet, Palaiseau, France.
[b]Also at Università di Milano Bicocca, Milano, Italy.
[c]Also at Università di Modena e Reggio Emilia, Modena, Italy.
[d]Also at Novosibirsk State University, Novosibirsk, Russia.
[e]Also at Università di Ferrara, Ferrara, Italy.
[f]Also at LIFAELS, La Salle, Universitat Ramon Llull, Barcelona, Spain.
[g]Also at Università di Bologna, Bologna, Italy.
[h]Also at Università di Genova, Genova, Italy.
[i]Also at Università di Pisa, Pisa, Italy.
[j]Also at Università di Bari, Bari, Italy.
[k]Also at Sezione INFN di Trieste, Trieste, Italy.
[l]Also at Università degli Studi di Milano, Milano, Italy.
[m]Also at Universidade Federal do Triângulo Mineiro (UFTM), Uberaba-MG, Brazil.
[n]Also at AGH - University of Science and Technology, Faculty of Computer Science, Electronics and Telecommunications, Kraków, Poland.
[o]Also at Università di Padova, Padova, Italy.
[p]Also at Università di Cagliari, Cagliari, Italy.
[q]Also at MSU - Iligan Institute of Technology (MSU-IIT), Iligan, Philippines.
[r]Also at Escuela Agrícola Panamericana, San Antonio de Oriente, Honduras.
[s]Also at Scuola Normale Superiore, Pisa, Italy.
[t]Also at Hanoi University of Science, Hanoi, Vietnam.
[u]Also at P.N. Lebedev Physical Institute, Russian Academy of Science (LPI RAS), Moscow, Russia.
[v]Also at National Research University Higher School of Economics, Moscow, Russia.
[w]Also at Università di Roma Tor Vergata, Roma, Italy.
[x]Also at Università di Roma La Sapienza, Roma, Italy.
[y]Also at Università della Basilicata, Potenza, Italy.
[z]Also at Università di Urbino, Urbino, Italy.
[aa]Also at Physics and Micro Electronic College, Hunan University, Changsha City, China.
[bb]Also at School of Physics and Information Technology, Shaanxi Normal University (SNNU), Xi'an, China.